Tunable Superconducting Coupling of Quantum Dots via Andreev Bound States in Semiconductor-Superconductor Nanowires

Chun-Xiao Liu, * Guanzhong Wang, Tom Dvir, and Michael Wimmer
Qutech and Kavli Institute of Nanoscience, Delft University of Technology, Delft 2600 GA, Netherlands

(Received 3 March 2022; revised 18 May 2022; accepted 23 November 2022; published 20 December 2022)

Semiconductor quantum dots have proven to be a useful platform for quantum simulation in the solid state. However, implementing a superconducting coupling between quantum dots mediated by a Cooper pair has so far suffered from limited tunability and strong suppression. This has limited applications such as Cooper pair splitting and quantum dot simulation of topological Kitaev chains. In this Letter, we propose how to mediate tunable effective couplings via Andreev bound states in a semiconductor-superconductor nanowire connecting two quantum dots. We show that in this way it is possible to individually control both the coupling mediated by Cooper pairs and by single electrons by changing the properties of the Andreev bound states with easily accessible experimental parameters. In addition, the problem of coupling suppression is greatly mitigated. We also propose how to experimentally extract the coupling strengths from resonant current in a three-terminal junction. Our proposal will enable future experiments that have not been possible so far.

DOI: 10.1103/PhysRevLett.129.267701

Introduction.—Semiconductor quantum dots [1–3] have proven to be a useful platform for quantum simulation in the solid state [4–6]. Controlling dot levels and the transfer of single electrons between dots [7–10] allows us to engineer synthetic Hamiltonians such that the desired functionality is achieved, for example, allowing for spin qubit operations [11–16], or simulating the Fermi-Hubbard model [17–19] or exotic magnetism [20–25].

Adding a superconducting coupling between quantum dots, i.e., a coupling mediated by a Cooper pair instead of single electrons only, would extend the range of possible Hamiltonians tremendously. Examples include operations on Andreev qubits [26–30], or implementing exotic superconducting systems such as a topological Kitaev chain [31–33], which might be utilized to implement topological quantum computation [34–41].

The basic building block for such a simulation is the coupling between two quantum dots. In fact, the coupling between two quantum dots mediated by a Cooper pair is of an intrinsic interest for fundamental physics itself: used as a Cooper pair splitter, the electrons of the Cooper pair are separated in space while maintaining quantum entanglement [42–47], which can be used to perform the Bell inequality test [48–50] and has potential applications in quantum teleportation [51] and quantum cryptography [52,53]. Despite much experimental progress [54–70], the splitting efficiency of Cooper pair splitters nowadays is still not high enough for the Bell inequality test. In addition, a sufficient control of the superconducting coupling between two quantum dots, the prerequisite for quantum simulation, has not been demonstrated experimentally. To proceed, a method of controlling superconducting and single electron coupling independently is dearly needed.

In most of the existing proposals and experiments, the couplings between quantum dots are mediated by the quasiparticle continuum of the superconductor [31,42,44,46,71]. The disadvantage of this approach is the limited tunability, as the electronic properties of the superconducting continuum cannot be controlled experimentally. Moreover, the coupling strengths between dots are strongly suppressed when using metallic superconductors.

In this Letter, we propose to mediate tunable effective couplings via Andreev bound states in a semiconductor-superconductor nanowire connecting two quantum dots, based on the fact that control over hybrid nanowires has been demonstrated experimentally, e.g., by tuning a nearby electrostatic gate [72]. We show that in this way it is possible to individually control both the coupling mediated by Cooper pairs and by single electrons by changing the properties of the Andreev bound states with easily accessible experimental parameters. In addition, the problem of coupling suppression is greatly mitigated. Finally, we propose how to experimentally extract the coupling strengths from resonant current in a three-terminal junction, allowing for an experimental verification of our theory [73].

Model and Hamiltonian.—The system consists of two quantum dots connected by a semiconductor-superconductor nanowire, see Fig. 1(a). The Hamiltonian is

$$\begin{aligned} H &= H_S + H_D + H_{SD}, \\ H_S &\approx E_1\gamma_1^\dagger\gamma_1 + E_2\gamma_2^\dagger\gamma_2, \\ H_D &= \varepsilon_l d_{l\eta}^\dagger d_{l\eta} + \varepsilon_r d_{r\sigma}^\dagger d_{r\sigma}, \\ H_{SD} &= -t_l c_{x_l\eta}^\dagger d_{l\eta} - t_r c_{x_r\sigma}^\dagger d_{r\sigma} + \text{H.c.} \end{aligned} \tag{1}$$

Here, H_S is the Hamiltonian for the hybrid nanowire of length $L = x_r - x_l$. In the short-wire limit where the level spacing is larger than the superconducting gap, we consider only two normal states closest to the Fermi energy (which form a Kramers' pair in the presence of time-reversal invariance). With an induced s-wave pairing, the normal states are gapped and become two Andreev bound states defined as $\gamma_i^\dagger = \sum_{x,s=\uparrow,\downarrow}[u_i(xs)c_{xs}^\dagger + v_i(xs)c_{xs}]$, where the wave functions and excitation energies are obtained by solving the Bogoliubov–de Gennes equation $h_{\mathrm{BdG}}(x)(u_i, v_i)^\intercal = E_i(u_i, v_i)^\intercal$. H_D describes two quantum dots. In the limit of strong Zeeman splitting and Coulomb interaction, i.e.,

$$\varepsilon_{l,r} < g_{\mathrm{dot}}\mu_B B, U, \qquad g_{\mathrm{dot}}\mu_B B < \delta E_{\mathrm{dot}}, \tag{2}$$

each quantum dot accommodates only a single spin-polarized level near Fermi energy [3,74], with the polarization axes of the two dots being the same and parallel to a globally applied magnetic field. Here, a large dot level spacing δE_{dot} guarantees that adjacent levels are spin-up and spin-down states from the same orbital. The spin indices η, σ in Eq. (1) can be either $\uparrow$ or $\downarrow$, but no summation is taken on them because the dots are in the spin-polarized regime. H_{SD} describes the spin-conserved electron tunneling between dots and the ends of the nanowire at $x = x_{l,r}$.

Such setups of two normal dots coupled by a proximitized nanowire segment, i.e., a proximitized central quantum dot, have been studied before experimentally and theoretically in the context of Cooper pair splitting, e.g., in Refs. [65,75]. In contrast, our focus will be on using the Andreev bound state in the central segment to control the effective coupling of the outer dots.

Effective couplings between dots.—In the tunneling limit $t_{l,r} < \Delta$, we can apply a Schrieffer-Wolff transformation to obtain an effective Hamiltonian for the coupled quantum dots. That is, $H_{\mathrm{eff}} = H_D + H_{\mathrm{interdot}}$, with

$$\begin{aligned} H_{\mathrm{interdot}} &= -PH_{SD}\frac{(1-P)}{H_S + H_D}H_{SD}P + O(t_{l,r}^3/\Delta^2) \\ &= -\Gamma_{\eta\sigma}^{\mathrm{CAR}} d_{l\eta}^\dagger d_{r\sigma}^\dagger - \Gamma_{\eta\sigma}^{\mathrm{ECT}} d_{l\eta}^\dagger d_{r\sigma} + \mathrm{H.c.} \end{aligned} \tag{3}$$

Here, P is the projection operator onto the ground state of the uncoupled dot-superconductor system. $\Gamma_{\eta\sigma}^{\mathrm{CAR}}$ and $\Gamma_{\eta\sigma}^{\mathrm{ECT}}$ are the Andreev bound states-mediated effective couplings between two spin-polarized dot levels, with

$$\begin{aligned} \Gamma_{\eta\sigma}^{\mathrm{CAR}} &= \frac{t_l t_r}{\Delta}\sum_{m=1,2}\frac{u_m(x_l\eta)v_m^*(x_r\sigma) - u_m(x_r\sigma)v_m^*(x_l\eta)}{E_m/\Delta}, \\ \Gamma_{\eta\sigma}^{\mathrm{ECT}} &= \frac{t_l t_r}{\Delta}\sum_{m=1,2}\frac{u_m(x_l\eta)u_m^*(x_r\sigma) - v_m(x_r\sigma)v_m^*(x_l\eta)}{E_m/\Delta}. \end{aligned} \tag{4}$$

Here, $\Gamma_{\eta\sigma}^{\mathrm{CAR}}$ is a superconducting effective coupling, and physically is induced by a coherent crossed Andreev reflection (CAR) process, where an incoming electron with spin σ from the right dot is reflected nonlocally into a hole with spin η in the left dot [Fig. 1(b)]. On the other hand, $\Gamma_{\eta\sigma}^{\mathrm{ECT}}$ is a normal effective coupling, and is induced by elastic cotunneling (ECT), where a single electron hops from the right dot to the left via the Andreev bound states [Fig. 1(c)]. Equation (4) is the most general expression. In what follows, we will define $P_{\eta\sigma}^a = |\Gamma_{\eta\sigma}^a\Delta/(t_l t_r)|^2$ to characterize the coupling strength, and analyze its dependence on the physical parameters of the Andreev bound states. As we will see, $P_{\eta\sigma}^a$ is proportional to the experimentally measurable current $I_{\eta\sigma}^a$.

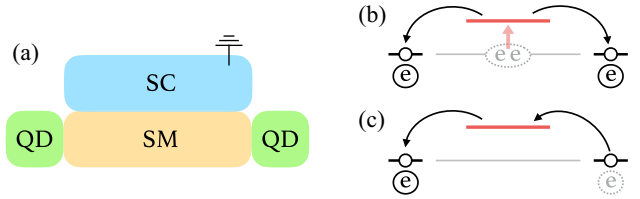

FIG. 1. Left: (a) Schematic of the device. Two separate quantum dots are connected by a short hybrid nanowire, which hosts Andreev bound states. Right: (b) Schematic of cross Andreev reflection and (c) elastic cotunneling. The red (black) horizontal line denotes the Andreev bound state (dot level), and the gray line represents the Fermi energy of the superconductor.

Energy and angle dependence.—We first consider a time-reversal invariant hybrid nanowire. Physically, this corresponds to a situation where the induced Zeeman splitting in the hybrid segment is negligible compared to the spin-orbit interaction or induced superconducting gap. The excitation energies of the degenerate Andreev bound states are $E_{1,2} = E_n = \sqrt{\xi_n^2 + \Delta^2}$ with $\xi_n = \varepsilon_n - \mu$ being the normal-state energy. The Bogoliubov–de Gennes wave functions are $u_1(x\sigma) = u_0\psi_n(x\sigma)$, $v_1 = v_0\psi_{\bar{n}}^*$, and $u_2 = -u_0\psi_{\bar{n}}$, $v_2 = v_0\psi_n^*$, where $\psi_n, \psi_{\bar{n}}$ are the normal-state wave functions, and $u_0^2 = 1 - v_0^2 = 1/2 + \xi_n/2E_n$ are coherence factors. From Eq. (4), we then obtain

$$\begin{aligned} P_{\eta\sigma}^{\mathrm{CAR}} &= \mathcal{C}_0(\xi_n/\Delta)|\psi_n(x_l\eta)\psi_{\bar{\eta}}(x_r\sigma) - \psi_n(x_r\sigma)\psi_{\bar{\eta}}(x_l\eta)|^2, \\ P_{\eta\sigma}^{\mathrm{ECT}} &= \mathcal{E}_0(\xi_n/\Delta)|\psi_n(x_l\eta)\psi_n^*(x_r\sigma) + \psi_{\bar{\eta}}(x_l\eta)\psi_{\bar{n}}^*(x_r\sigma)|^2, \end{aligned} \tag{5}$$

where $\mathcal{C}_0(z) = [2u_0v_0/(E_n/\Delta)]^2 = (z^2+1)^{-2}$, $\mathcal{E}_0(z) = [(u_0^2 - v_0^2)/(E_n/\Delta)]^2 = z^2(z^2+1)^{-2}$ with $z = \xi_n/\Delta$. Equation (5) shows that P^a has a separable dependence on the energy ξ_n and on the wave functions $\psi_{n,\bar{n}}$ of the bound states. In particular, the energy dependence is universal because it only depends on the coherence factors u_0 and v_0. This is a consequence of time reversal symmetry and holds for any hybrid structure, thus not only for one-dimensional wires. As shown in Fig. 2(a), $\mathcal{C}_0(z)$ of crossed Andreev reflection has a single peak centered at $z = 0$

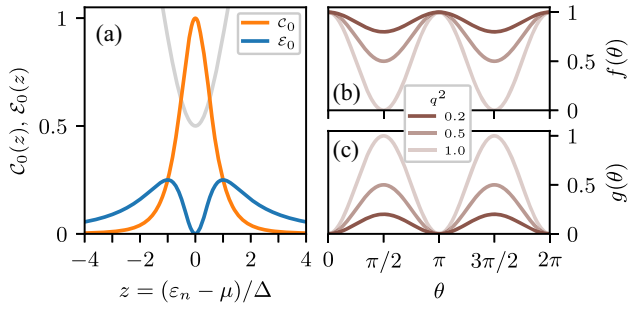

FIG. 2. Energy and angle dependence of P^a for a time-reversal invariant hybrid nanowire. (a) CAR (orange) and ECT (blue) profiles as a function of the normal-state energy z. The gray line denotes the excitation energy $E_m/\Delta = \sqrt{z^2+1}$ of the Andreev bound states (for better visual effect we shift $E_m/\Delta \to E_m/\Delta - 1/2$). Right panels: angle dependence of P^a in favorable (b) and unfavorable (c) channels, with θ the angle between the spin-orbit field in the hybrid nanowire and the global magnetic field. Here, $q^2 = \sin^2(k_{\rm SO}L)$ characterizes the amount of spin precession through the nanowire due to spin-orbit interaction.

($\xi_n = 0$) and decays as z^{-4} at large $|z|$, while $\mathcal{E}_0(z)$ of elastic cotunneling has double peaks located at $z = \pm 1$, and decays as z^{-2} at large $|z|$. Interestingly, $\mathcal{E}_0(z)$ has a dip at $z = 0$ due to destructive interference between two virtual paths with a π-phase shift. The strikingly different profiles of $\mathcal{C}_0(z)$ and $\mathcal{E}_0(z)$ is the first main finding in this Letter, which indicates that one can vary the relative CAR and ECT amplitudes by changing the chemical potential of the Andreev bound state. For the wave function part in Eq. (5), time-reversal invariance, i.e., $\psi_{\bar{n}}(x\sigma) = \mathcal{T}\psi_n(x\sigma) = -i\sigma_y\psi_n^*(x\sigma)$, gives the following symmetry relations between different dot-spin channels:

$$P^a_{\uparrow\uparrow} = P^a_{\downarrow\downarrow}, \qquad P^a_{\uparrow\downarrow} = P^a_{\downarrow\uparrow}, \tag{6}$$

for both CAR and ECT. Thus, we will focus on only two spin channels $\uparrow\uparrow$ and $\uparrow\downarrow$ in the following discussions.

If spin-orbit field is the only spinful field in the hybrid nanowire and has a constant direction, we can find the angle dependence in P^a explicitly. In the specific case of a one-dimensional Rashba spin-orbit interaction with strength α_R [76], the wave functions take the form of $\psi_n(x) = \phi_n(x)e^{-ik_{\rm so}x\sigma_{\rm so}}(1,0)^{\intercal}$, where $\phi_n(x)$ is the eigenfunction in the absence of spin-orbit interaction, $k_{\rm so} = m\alpha_R/\hbar^2$ is the spin-orbit wave vector, and $\sigma_{\rm so} = \cos\theta\sigma_z + \sin\theta\sigma_x$ is the spin-orbit field which has an angle θ from the magnetic field. Here, without loss of generality, we fix the magnetic field (i.e., dot spin axis) along z and rotate the spin-orbit field in the xz plane. Plugging the wave functions into Eq. (5), we obtain

$$\begin{aligned} \tilde{P}^{\rm CAR}_{\uparrow\uparrow} &= \mathcal{C}_0(z)\, g(\theta), \qquad \tilde{P}^{\rm CAR}_{\uparrow\downarrow} = \mathcal{C}_0(z)\, f(\theta), \\ \tilde{P}^{\rm ECT}_{\uparrow\uparrow} &= \mathcal{E}_0(z)\, f(\theta), \qquad \tilde{P}^{\rm ECT}_{\uparrow\downarrow} = \mathcal{E}_0(z)\, g(\theta), \end{aligned} \tag{7}$$

where $f(\theta) = p^2 + q^2\cos^2\theta$ and $g(\theta) = q^2\sin^2\theta$. Here, $p = \cos(k_{\rm so}L)$ and $q = \sin(k_{\rm so}L)$ characterize the amount of spin precession through the nanowire due to spin-orbit interaction, with $p^2 + q^2 = 1$. Note that in Eq. (7), we have defined a renormalized $\tilde{P}^a_{\eta\sigma} = P^a_{\eta\sigma}/|\phi_n^2(x_l)\phi_n^2(x_r)|$. The details of the orbital wave function $\phi_n(x)$ (and thus, e.g., details of the potential landscape or disorder) determine the overall coupling strengths but do not affect the relative CAR and ECT amplitudes. As a result, the renormalized $\tilde{P}^a$ relies only on the *general* properties of Andreev bound states, i.e., coherence factors u_0, v_0, spin-orbit coupling $k_{\rm so}$, and induced Zeeman spin splitting E_Z. As shown in Figs. 2(b) and 2(c), $\tilde{P}^a$ has a sinusoidal dependence on the angle θ. In particular, CAR-$\uparrow\downarrow$ and ECT-$\uparrow\uparrow$ are more favorable channels with $f(\theta) \geq p^2$. By contrast, CAR-$\uparrow\uparrow$ and ECT-$\uparrow\downarrow$ vanish at $\theta = 0$ or π due to spin conservation. Hence, in order to have CAR and ECT couplings simultaneously finite in a particular dot spin channel, it is crucial to have a finite spin-orbit field misaligned with the magnetic field. More surprisingly, although $\tilde{P}^a_{\eta\sigma}$ has a strong energy dependence, the ratio of angle-averaged $\tilde{P}^a$ in unfavorable and favorable channels depends only on the amount of spin precession, i.e.,

$$\frac{\langle\tilde{P}^{\rm CAR}_{\uparrow\uparrow}\rangle}{\langle\tilde{P}^{\rm CAR}_{\uparrow\downarrow}\rangle} = \frac{\langle\tilde{P}^{\rm ECT}_{\uparrow\downarrow}\rangle}{\langle\tilde{P}^{\rm ECT}_{\uparrow\uparrow}\rangle} = \frac{\sin^2(k_{\rm so}L)}{2-\sin^2(k_{\rm so}L)}, \tag{8}$$

with $\langle\tilde{P}^a_{\eta\sigma}\rangle = (2\pi)^{-1}\int_0^{2\pi} d\theta\, \tilde{P}^a_{\eta\sigma}(\theta)$. This provides a new way to extract the strength of induced spin-orbit coupling in the hybrid nanowire.

Effect of Zeeman spin splitting.—We now consider the effect of induced Zeeman splitting in the hybrid segment. This relaxes the assumption of time-reversal invariance, provides an additional experimentally accessible parameter to tune the profiles of CAR and ECT, and allows for an additional comparison between experiment and theory. The direction of the Zeeman field is parallel to the spin-polarization axis in dots, i.e., $E_Z\sigma_z$, because we have assumed a globally applied magnetic field in the system. However, the magnitude of the Zeeman energy may be different between dots and the hybrid segment because of renormalization effects due to the metallic superconductor [77]. We assume weak spin-orbit interaction $k_{\rm SO}L \ll 1$ and $E_Z < \Delta$. Under these assumptions, the energies of the Andreev bound states become $E_{1,2} \approx \sqrt{\xi_n^2 + \Delta^2} \pm E_Z$, while the wave functions remain the same as those in the time-reversal invariant scenario [74]. We thus obtain

$$\begin{aligned} \tilde{P}^{\rm CAR}_{\uparrow\uparrow}(\delta) &= \tilde{P}^{\rm CAR}_{\downarrow\downarrow}(\delta) = (z^2+1-\delta^2)^{-2}\, q^2\sin^2\theta, \\ \tilde{P}^{\rm CAR}_{\uparrow\downarrow}(\delta) &= \tilde{P}^{\rm CAR}_{\downarrow\uparrow}(\delta) = (z^2+1-\delta^2)^{-2}\,(p^2 + q^2\cos^2\theta), \\ \tilde{P}^{\rm ECT}_{\uparrow\uparrow}(\delta) &= \tilde{P}^{\rm ECT}_{\downarrow\downarrow}(-\delta) = \frac{(pz-\delta')^2 + q^2\cos^2\theta\,(z-\delta)^2}{(z^2+1-\delta^2)^2}, \\ \tilde{P}^{\rm ECT}_{\uparrow\downarrow}(\delta) &= \tilde{P}^{\rm ECT}_{\downarrow\uparrow}(\delta) = \frac{q^2z^2 + \delta^2\cos^2\theta\,(1-p)^2}{(z^2+1-\delta^2)^2}\sin^2\theta, \end{aligned} \tag{9}$$

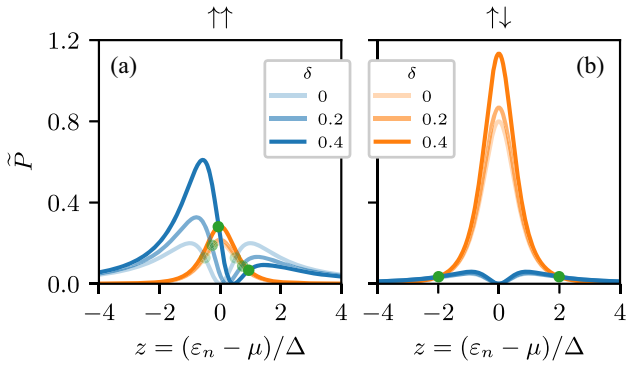

FIG. 3. Effects of Zeeman spin splitting on CAR (orange) and ECT (blue) profiles in equal-spin (a) and opposite-spin (b) channels. $\tilde{P}^{\mathrm{CAR}}_{\uparrow\uparrow}$, $\tilde{P}^{\mathrm{CAR}}_{\uparrow\downarrow}$, and $\tilde{P}^{\mathrm{ECT}}_{\uparrow\downarrow}$ all increase with E_Z, with their profiles remaining symmetric about $z = 0$. The profile of $\tilde{P}^{\mathrm{ECT}}_{\uparrow\uparrow}$ becomes asymmetric when $E_Z > 0$, with one peak being lifted and the other suppressed. Green dots indicate where $\tilde{P}^{\mathrm{CAR}} = \tilde{P}^{\mathrm{ECT}}$ for particular values of δ. Here, we choose $q^2 = 0.2$ and $\theta = \pi/2$, corresponding to the realistic device investigated in Ref. [73].

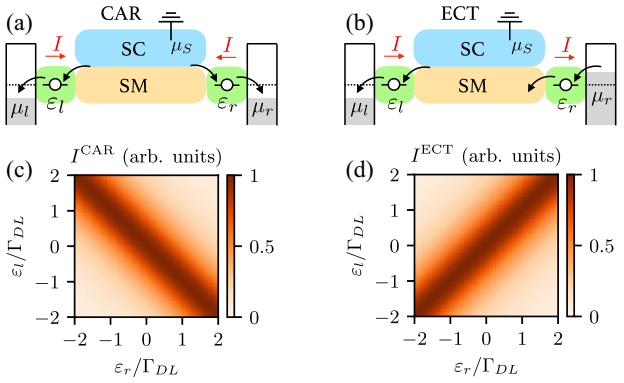

FIG. 4. (a) and (b) Schematic for the three-terminal junctions. (c) and (d) Resonant current in the $(\varepsilon_l, \varepsilon_r)$ plane. The currents have a Breit-Wigner resonance form, with the broadening width being the dot-lead coupling strength Γ_{DL}. CAR and ECT current assumes the maximum value I^a_{max} when $\varepsilon_l = \pm\varepsilon_r$, respectively. The strengths of the effective couplings can be extracted by $\Gamma^a = \sqrt{I^a_{\mathrm{max}}\Gamma_{DL}\hbar/e}$.

where $\delta = E_Z/\Delta < 1$ and $\delta' = \delta(p\cos^2\theta + \sin^2\theta)$. As shown in Fig. 3, $\tilde{P}^{\mathrm{CAR}}_{\uparrow\uparrow}$, $\tilde{P}^{\mathrm{CAR}}_{\uparrow\downarrow}$, and $\tilde{P}^{\mathrm{ECT}}_{\uparrow\downarrow}$ all increase with E_Z, with their profiles remaining symmetric about $z = 0$, while $\tilde{P}^{\mathrm{ECT}}_{\uparrow\uparrow}$ becomes asymmetric, with one peak being lifted and the other suppressed. In addition, the green dots in Fig. 3 show where $\tilde{P}^{\mathrm{CAR}} = \tilde{P}^{\mathrm{ECT}}$ for particular values of δ, corresponding to the sweet spots in a minimal Kitaev chain. Such a sweet spot can be found in general because ECT is larger than CAR at large $|z|$ and goes to zero near $z = 0$, guaranteeing the crossing of the two curves in most experimentally relevant parameter regimes.

Extracting Γ^a experimentally.—To reach the optimal parameter regime for the desired application, it is necessary to be able to extract the strengths of the effective interdot couplings experimentally. For this purpose, we propose a three-terminal junction, where two quantum dots are now connected with two external normal electrodes, respectively [Figs. 4(a) and 4(b)]. The strengths of $\Gamma^{\mathrm{CAR/ECT}}$ can be extracted from resonant current.

Our considerations and calculations follow those in Refs. [42,43], which focused on the current due to crossed Andreev reflection in a similar setup. Compared to the previous works, the differences made in our calculations include the following. (1) We now consider Andreev bound states instead of quasiparticle continuum in the superconducting segment. (2) Spin-orbit interaction in the hybrid segment breaks spin conservation. (3) Currents become spin selective. (4) We generalize the calculations to elastic cotunneling scenarios.

The total Hamiltonian for the three-terminal junction, as shown in Fig. 4, is $H_{\mathrm{tot}} = H + H_L + H_{DL}$. H is the dot-superconductor-dot system introduced by Eq. (1). $H_L = \sum_k (\varepsilon_k - \mu_l) a^\dagger_{lk\eta} a_{lk\eta} + (\varepsilon_k - \mu_r) a^\dagger_{rk\sigma} a_{rk\sigma}$ are the normal leads, which are conventional Fermi liquids with electrons filled up to the Fermi energy $\mu_{l,r}$. $H_{DL} = \sum_k (-t'_l d^\dagger_{l\eta} a_{lk\eta} - t'_r d^\dagger_{r\sigma} a_{rk\sigma}) + \mathrm{H.c.}$ describes the dot-lead tunneling. The relevant parameter regime for generating resonant current is [42,43]

$$\Gamma_{DL}, k_B T < \delta\mu < \Delta, g_{\mathrm{dot}}\mu_B B, U,$$
$$\varepsilon_l, \varepsilon_r, \Gamma_{SD} < \Gamma_{DL}. \tag{10}$$

Here, $\delta\mu$ is the applied bias voltage, with $\delta\mu = \mu_S - \mu_{l,r} > 0$ for generating CAR current [Fig. 4(a)], and $\delta\mu/2 = \mu_r - \mu_S = \mu_S - \mu_l > 0$ for ECT [Fig. 4(b)]. Bias voltage is smaller than the induced gap Δ, dot charging energy U, and dot Zeeman splitting $g_{\mathrm{dot}}\mu_B B$, such that undesired processes such as local Andreev reflection and inelastic cotunneling would be suppressed, and that the current become spin selective. On the other hand, the bias voltage window should be large enough to include the full width of the broadened dot states, i.e., $\delta\mu > \Gamma_{DL} = \pi\nu(|t'_l|^2 + |t'_r|^2)$ with ν being the lead density of states. The dot-lead coupling should be stronger than the superconductor-dot coupling $\Gamma_{DL} > \Gamma_{SD} \approx t_{ln} t_{rn}/\Delta$, such that the quick interdot tunneling process maintains coherence. Additionally, dot energies need to be tuned close to the superconducting Fermi energy to make dot levels on resonance. Once all these criteria are met, resonant current will flow between source and drain leads.

The resonant currents are calculated using the rate equation altogether with the T-matrix approach [42,43,74,78]. When $\mu_S > \mu_{l,r}$, Cooper pairs from the superconducting lead would split into two electrons, which flow to two separate normal leads via dots, respectively, giving the following spin-selective CAR current

$$I_{\eta\sigma}^{\mathrm{CAR}} = \frac{e}{\hbar} \cdot \frac{\Gamma_{DL}^2}{(\varepsilon_l + \varepsilon_r)^2 + \Gamma_{DL}^2} \cdot \frac{|\Gamma_{\eta\sigma}^{\mathrm{CAR}}|^2}{\Gamma_{DL}}, \tag{11}$$

with $\Gamma_{\eta\sigma}^{\mathrm{CAR}}$ being the effective coupling defined in Eq. (4). As shown in Fig. 4(c), in the $(\varepsilon_l, \varepsilon_r)$ plane CAR current has a Breit-Wigner resonance form with broadening width Γ_{DL}, and reaches the maximum value along $\varepsilon_l = -\varepsilon_r$ due to energy conservation. In exactly the same setup but with a different bias voltage: $\mu_l < \mu_S < \mu_r$, now a single electron flows from one to the other normal lead, giving the spin-selective ECT current

$$I_{\eta\sigma}^{\mathrm{ECT}} = \frac{e}{\hbar} \cdot \frac{\Gamma_{DL}^2}{(\varepsilon_l - \varepsilon_r)^2 + \Gamma_{DL}^2} \cdot \frac{|\Gamma_{\eta\sigma}^{\mathrm{ECT}}|^2}{\Gamma_{DL}}, \tag{12}$$

where $\Gamma_{\eta\sigma}^{\mathrm{ECT}}$ is defined in Eq. (4). The ECT current has the same Breit-Wigner form, but now assumes the maximum value when $\varepsilon_l = \varepsilon_r$, as shown in Fig. 4(d). Equations (11) and (12) indicate that resonant current is proportional to the square of the corresponding interdot coupling strength. Thus, experimentally one can extract the strengths using the formula $\Gamma^a = \sqrt{I_{\mathrm{max}}^a \Gamma_{DL} \hbar / e}$, where Γ_{DL} is read off from the resonance broadening width in gate voltage times the lever arm, and I_{max}^a is the current value along $\varepsilon_l = -\varepsilon_r$ for CAR and $\varepsilon_l = \varepsilon_r$ for ECT.

Discussions.—We have given a proposal for mediating tunable superconducting and normal couplings of quantum dots via Andreev bound states. This provides an experimentally accessible method for fine-tuning the physical system into the desirable parameter regime. In particular, the Cooper pair splitting efficiency now can be enhanced by tuning the energy close to $z = 0$ in Fig. 2(a), where the crossed Andreev reflection is strengthened and simultaneously the unwanted elastic cotunneling processes are strongly suppressed. On the other hand, a minimal Kitaev chain, which is composed of two spin-polarized dots, now becomes tunable and can host Majorana zero modes. In practice, this tuning protocol can be implemented by controlling the electrostatic gate near the semiconductor-superconductor segment to change the chemical potential therein, eliminating the need of noncollinear magnetic fields [32]. This makes our proposal especially appealing, since all the necessary ingredients, i.e., spin-polarized quantum dots [79], gated hybrid nanowire with spin-orbit interaction [72,80], are within reach of existing materials and technologies. We thus expect that our proposal will enable future experiments that have not been possible so far. In fact, in a recent experiment we and our co-workers have already shown a record high Cooper pair splitting efficiency enabled by coupling through Andreev bound states [73]. Also, a tunable Kitaev chain of two sites has been experimentally realized [81], providing an exciting platform for studying topological superconductivity and non-Abelian statistics.

This work was supported by a subsidy for top consortia for knowledge and innovation (TKl toeslag), by the Dutch Organization for Scientific Research (NWO), by the Foundation for Fundamental Research on Matter (FOM) and by Microsoft Corporation Station Q.

C.-X. L. formulated the project idea with input from G. W. and T. D., and designed the project; C.-X. L. performed the calculations with input from M. W.; C.-X. L. and M. W. wrote the manuscript with input from all authors.

*Corresponding author.
chunxiaoliu62@gmail.com

[1] L. P. Kouwenhoven, D. G. Austing, and S. Tarucha, Few-electron quantum dots, Rep. Prog. Phys. **64**, 701 (2001).
[2] W. G. van der Wiel, S. De Franceschi, J. M. Elzerman, T. Fujisawa, S. Tarucha, and L. P. Kouwenhoven, Electron transport through double quantum dots, Rev. Mod. Phys. **75**, 1 (2002).
[3] R. Hanson, L. P. Kouwenhoven, J. R. Petta, S. Tarucha, and L. M. K. Vandersypen, Spins in few-electron quantum dots, Rev. Mod. Phys. **79**, 1217 (2007).
[4] E. Manousakis, A quantum-dot array as model for copper-oxide superconductors: A dedicated quantum simulator for the many-fermion problem, J. Low Temp. Phys. **126**, 1501 (2002).
[5] Tim Byrnes, Na Young Kim, Kenichiro Kusudo, and Yoshihisa Yamamoto, Quantum simulation of Fermi-Hubbard models in semiconductor quantum-dot arrays, Phys. Rev. B **78**, 075320 (2008).
[6] Pierre Barthelemy and Lieven M. K. Vandersypen, Quantum dot systems: A versatile platform for quantum simulations, Ann. Phys. (Amsterdam) **525**, 808 (2013).
[7] F. H. L. Koppens, C. Buizert, K. J. Tielrooij, I. T. Vink, K. C. Nowack, T. Meunier, L. P. Kouwenhoven, and L. M. K. Vandersypen, Driven coherent oscillations of a single electron spin in a quantum dot, Nature (London) **442**, 766 (2006).
[8] Frederico Martins, Filip K. Malinowski, Peter D. Nissen, Edwin Barnes, Saeed Fallahi, Geoffrey C. Gardner, Michael J. Manfra, Charles M. Marcus, and Ferdinand Kuemmeth, Noise Suppression Using Symmetric Exchange Gates in Spin Qubits, Phys. Rev. Lett. **116**, 116801 (2016).
[9] M. D. Reed, B. M. Maune, R. W. Andrews, M. G. Borselli, K. Eng, M. P. Jura, A. A. Kiselev, T. D. Ladd, S. T. Merkel, I. Milosavljevic, E. J. Pritchett, M. T. Rakher, R. S. Ross, A. E. Schmitz, A. Smith, J. A. Wright, M. F. Gyure, and A. T. Hunter, Reduced Sensitivity to Charge Noise in Semiconductor Spin Qubits via Symmetric Operation, Phys. Rev. Lett. **116**, 110402 (2016).
[10] T. A. Baart, M. Shafiei, T. Fujita, C. Reichl, W. Wegscheider, and L. M. K. Vandersypen, Single-spin CCD, Nat. Nanotechnol. **11**, 330 (2016).
[11] Daniel Loss and David P. DiVincenzo, Quantum computation with quantum dots, Phys. Rev. A **57**, 120 (1998).
[12] D. P. DiVincenzo, D. Bacon, J. Kempe, G. Burkard, and K. B. Whaley, Universal quantum computation with the exchange interaction, Nature (London) **408**, 339 (2000).

[13] Jeremy Levy, Universal Quantum Computation with Spin-1/2 Pairs and Heisenberg Exchange, Phys. Rev. Lett. **89**, 147902 (2002).
[14] T. Hayashi, T. Fujisawa, H. D. Cheong, Y. H. Jeong, and Y. Hirayama, Coherent Manipulation of Electronic States in a Double Quantum Dot, Phys. Rev. Lett. **91**, 226804 (2003).
[15] J. R. Petta, A. C. Johnson, J. M. Taylor, E. A. Laird, A. Yacoby, M. D. Lukin, C. M. Marcus, M. P. Hanson, and A. C. Gossard, Coherent manipulation of coupled electron spins in semiconductor quantum dots, Science **309**, 2180 (2005).
[16] R. Mizuta, R. M. Otxoa, A. C. Betz, and M. F. Gonzalez-Zalba, Quantum and tunneling capacitance in charge and spin qubits, Phys. Rev. B **95**, 045414 (2017).
[17] J. Hubbard, Electron correlations in narrow energy bands, Proc. R. Soc. A **276**, 238 (1963).
[18] Shuo Yang, Xin Wang, and S. Das Sarma, Generic Hubbard model description of semiconductor quantum-dot spin qubits, Phys. Rev. B **83**, 161301(R) (2011).
[19] T. Hensgens, T. Fujita, L. Janssen, Xiao Li, C. J. Van Diepen, C. Reichl, W. Wegscheider, S. Das Sarma, and L. M. K. Vandersypen, Quantum simulation of a Fermi-Hubbard model using a semiconductor quantum dot array, Nature (London) **548**, 70 (2017).
[20] Yosuke Nagaoka, Ferromagnetism in a narrow, almost half-filled *s* band, Phys. Rev. **147**, 392 (1966).
[21] D. C. Mattis, Eigenvalues and magnetism of electrons on an artificial molecule, Int. J. Nanosci. **02**, 165 (2003).
[22] Erik Nielsen and R. N. Bhatt, Nanoscale ferromagnetism in nonmagnetic doped semiconductors, Phys. Rev. B **76**, 161202(R) (2007).
[23] Akira Oguri, Yunori Nisikawa, Yoshihide Tanaka, and Takahide Numata, Kondo screening of a high-spin Nagaoka state in a triangular quantum dot, J. Magn. Magn. Mater. **310**, 1139 (2007).
[24] J. von Stecher, E. Demler, M. D. Lukin, and A. M. Rey, Probing interaction-induced ferromagnetism in optical superlattices, New J. Phys. **12**, 055009 (2010).
[25] J. P. Dehollain, U. Mukhopadhyay, V. P. Michal, Y. Wang, B. Wunsch, C. Reichl, W. Wegscheider, M. S. Rudner, E. Demler, and L. M. K. Vandersypen, Nagaoka ferromagnetism observed in a quantum dot plaquette, Nature (London) **579**, 528 (2020).
[26] A. Zazunov, V. S. Shumeiko, E. N. Bratus', J. Lantz, and G. Wendin, Andreev Level Qubit, Phys. Rev. Lett. **90**, 087003 (2003).
[27] Nikolai M. Chtchelkatchev and Yu. V. Nazarov, Andreev Quantum Dots for Spin Manipulation, Phys. Rev. Lett. **90**, 226806 (2003).
[28] G. Wendin and V. S. Shumeiko, Quantum bits with Josephson junctions (review article), Low Temp. Phys. **33**, 724 (2007).
[29] C. Padurariu and Yu. V. Nazarov, Theoretical proposal for superconducting spin qubits, Phys. Rev. B **81**, 144519 (2010).
[30] S. Park and A. L. Yeyati, Andreev spin qubits in multichannel Rashba nanowires, Phys. Rev. B **96**, 125416 (2017).
[31] Jay D. Sau and S. Das Sarma, Realizing a robust practical Majorana chain in a quantum-dot-superconductor linear array, Nat. Commun. **3**, 964 (2012).
[32] Martin Leijnse and Karsten Flensberg, Parity qubits and poor man's Majorana bound states in double quantum dots, Phys. Rev. B **86**, 134528 (2012).
[33] Ion C Fulga, Arbel Haim, Anton R Akhmerov, and Yuval Oreg, Adaptive tuning of Majorana fermions in a quantum dot chain, New J. Phys. **15**, 045020 (2013).
[34] Chetan Nayak, Steven H. Simon, Ady Stern, Michael Freedman, and Sankar Das Sarma, Non-Abelian anyons and topological quantum computation, Rev. Mod. Phys. **80**, 1083 (2008).
[35] Jason Alicea, New directions in the pursuit of Majorana fermions in solid state systems, Rep. Prog. Phys. **75**, 076501 (2012).
[36] Martin Leijnse and Karsten Flensberg, Introduction to topological superconductivity and Majorana fermions, Semicond. Sci. Technol. **27**, 124003 (2012).
[37] C. W. J. Beenakker, Search for Majorana fermions in superconductors, Annu. Rev. Condens. Matter Phys. **4**, 113 (2013).
[38] Steven R. Elliott and Marcel Franz, Colloquium: Majorana fermions in nuclear, particle, and solid-state physics, Rev. Mod. Phys. **87**, 137 (2015).
[39] Sankar Das Sarma, Michael Freedman, and Chetan Nayak, Majorana zero modes and topological quantum computation, npj Quantum Inf. **1**, 15001 EP—(2015).
[40] D. A. Ivanov, Non-Abelian Statistics of Half-Quantum Vortices in *p*-Wave Superconductors, Phys. Rev. Lett. **86**, 268 (2001).
[41] Torsten Karzig, Christina Knapp, Roman M. Lutchyn, Parsa Bonderson, Matthew B. Hastings, Chetan Nayak, Jason Alicea, Karsten Flensberg, Stephan Plugge, Yuval Oreg, Charles M. Marcus, and Michael H. Freedman, Scalable designs for quasiparticle-poisoning-protected topological quantum computation with Majorana zero modes, Phys. Rev. B **95**, 235305 (2017).
[42] Patrik Recher, Eugene V. Sukhorukov, and Daniel Loss, Andreev tunneling, coulomb blockade, and resonant transport of nonlocal spin-entangled electrons, Phys. Rev. B **63**, 165314 (2001).
[43] Daniel Loss and Eugene V. Sukhorukov, Probing Entanglement and Nonlocality of Electrons in a Double-Dot via Transport and Noise, Phys. Rev. Lett. **84**, 1035 (2000).
[44] G. Falci, D. Feinberg, and F. W. J. Hekking, Correlated tunneling into a superconductor in a multiprobe hybrid structure, Europhys. Lett. **54**, 255 (2001).
[45] G. B. Lesovik, T. Martin, and G. Blatter, Electronic entanglement in the vicinity of a superconductor, Eur. Phys. J. B **24**, 287 (2001).
[46] D. Feinberg, Andreev scattering and cotunneling between two superconductor-normal metal interfaces: The dirty limit, Eur. Phys. J. B **36**, 419 (2003).
[47] Olivier Sauret, Denis Feinberg, and Thierry Martin, Quantum master equations for the superconductor–quantum dot entangler, Phys. Rev. B **70**, 245313 (2004).
[48] John S. Bell, On the problem of hidden variables in quantum mechanics, Rev. Mod. Phys. **38**, 447 (1966).
[49] N. M. Chtchelkatchev, Gianni Blatter, G. B. Lesovik, and Thierry Martin, Bell inequalities and entanglement in solid-state devices, Phys. Rev. B **66**, 161320(R) (2002).

[50] P. Samuelsson, E. V. Sukhorukov, and M. Büttiker, Orbital Entanglement and Violation of Bell Inequalities in Mesoscopic Conductors, Phys. Rev. Lett. **91**, 157002 (2003).

[51] Charles H. Bennett, Gilles Brassard, Claude Crépeau, Richard Jozsa, Asher Peres, and William K. Wootters, Teleporting an Unknown Quantum State via Dual Classical and Einstein-Podolsky-Rosen Channels, Phys. Rev. Lett. **70**, 1895 (1993).

[52] Artur K. Ekert, Quantum cryptography and Bell's theorem, in *Quantum Measurements in Optics*, edited by Paolo Tombesi and Daniel F. Walls (Springer, Boston, 1992), pp. 413–418.

[53] Nicolas Gisin, Grégoire Ribordy, Wolfgang Tittel, and Hugo Zbinden, Quantum cryptography, Rev. Mod. Phys. **74**, 145 (2002).

[54] D. Beckmann, H. B. Weber, and H. V. Löhneysen, Evidence for Crossed Andreev Reflection in Superconductor-Ferromagnet Hybrid Structures, Phys. Rev. Lett. **93**, 197003 (2004).

[55] S. Russo, M. Kroug, T. M. Klapwijk, and A. F. Morpurgo, Experimental Observation of Bias-Dependent Nonlocal Andreev Reflection, Phys. Rev. Lett. **95**, 027002 (2005).

[56] L. Hofstetter, S. Csonka, J. Nygård, and C. Schönenberger, Cooper pair splitter realized in a two-quantum-dot Y-junction, Nature (London) **461**, 960 (2009).

[57] L. G. Herrmann, F. Portier, P. Roche, A. L. Yeyati, T. Kontos, and C. Strunk, Carbon Nanotubes as Cooper-Pair Beam Splitters, Phys. Rev. Lett. **104**, 026801 (2010).

[58] Jian Wei and V. Chandrasekhar, Positive noise cross-correlation in hybrid superconducting and normal-metal three-terminal devices, Nat. Phys. **6**, 494 (2010).

[59] L. Hofstetter, S. Csonka, A. Baumgartner, G. Fülöp, S. d'Hollosy, J. Nygård, and C. Schönenberger, Finite-Bias Cooper Pair Splitting, Phys. Rev. Lett. **107**, 136801 (2011).

[60] J. Schindele, A. Baumgartner, and C. Schönenberger, Near-Unity Cooper Pair Splitting Efficiency, Phys. Rev. Lett. **109**, 157002 (2012).

[61] L. G. Herrmann, P. Burset, W. J. Herrera, F. Portier, P. Roche, C. Strunk, A. Levy Yeyati, and T. Kontos, Spectroscopy of non-local superconducting correlations in a double quantum dot, arXiv:1205.1972.

[62] Anindya Das, Yuval Ronen, Moty Heiblum, Diana Mahalu, Andrey V. Kretinin, and Hadas Shtrikman, High-efficiency Cooper pair splitting demonstrated by two-particle conductance resonance and positive noise cross-correlation, Nat. Commun. **3**, 1165 (2012).

[63] G. Fülöp, S. d'Hollosy, A. Baumgartner, P. Makk, V. A. Guzenko, M. H. Madsen, J. Nygård, C. Schönenberger, and S. Csonka, Local electrical tuning of the nonlocal signals in a Cooper pair splitter, Phys. Rev. B **90**, 235412 (2014).

[64] Z. B. Tan, D. Cox, T. Nieminen, P. Lähteenmäki, D. Golubev, G. B. Lesovik, and P. J. Hakonen, Cooper Pair Splitting by Means of Graphene Quantum Dots, Phys. Rev. Lett. **114**, 096602 (2015).

[65] G. Fülöp, F. Domínguez, S. d'Hollosy, A. Baumgartner, P. Makk, M. H. Madsen, V. A. Guzenko, J. Nygård, C. Schönenberger, A. Levy Yeyati, and S. Csonka, Magnetic Field Tuning and Quantum Interference in a Cooper Pair Splitter, Phys. Rev. Lett. **115**, 227003 (2015).

[66] I. V. Borzenets, Y. Shimazaki, G. F. Jones, M. F. Craciun, S. Russo, M. Yamamoto, and S. Tarucha, High efficiency CVD graphene-lead (Pb) Cooper pair splitter, Sci. Rep. **6**, 23051 (2016).

[67] L. E Bruhat, T. Cubaynes, J. J. Viennot, M. C. Dartiailh, M. M. Desjardins, A. Cottet, and T. Kontos, Circuit QED with a quantum-dot charge qubit dressed by Cooper pairs, Phys. Rev. B **98**, 155313 (2018).

[68] Z. B. Tan, A. Laitinen, N. S. Kirsanov, A. Galda, V. M. Vinokur, M. Haque, A. Savin, D. S. Golubev, G. B. Lesovik, and P. J. Hakonen, Thermoelectric current in a graphene Cooper pair splitter, Nat. Commun. **12**, 138 (2021).

[69] P. Pandey, R. Danneau, and D. Beckmann, Ballistic Graphene Cooper Pair Splitter, Phys. Rev. Lett. **126**, 147701 (2021).

[70] Antti Ranni, Fredrik Brange, Elsa T. Mannila, Christian Flindt, and Ville F. Maisi, Real-time observation of Cooper pair splitting showing strong non-local correlations, Nat. Commun. **12**, 6358 (2021).

[71] Martin Leijnse and Karsten Flensberg, Coupling Spin Qubits via Superconductors, Phys. Rev. Lett. **111**, 060501 (2013).

[72] Michiel W. A. de Moor, Jouri D. S. Bommer, Di Xu, Georg W. Winkler, Andrey E. Antipov, Arno Bargerbos, Guanzhong Wang, Nick van Loo, Roy L. M. Op het Veld, Sasa Gazibegovic, Diana Car, John A. Logan, Mihir Pendharkar, Joon Sue Lee, Erik P. A. M. Bakkers, Chris J. Palmstrøm, Roman M. Lutchyn, Leo P. Kouwenhoven, and Hao Zhang, Electric field tunable superconductor-semiconductor coupling in Majorana nanowires, New J. Phys. **20**, 103049 (2018).

[73] Guanzhong Wang, Tom Dvir, Grzegorz P. Mazur, Chun-Xiao Liu, Nick van Loo, Sebastiaan L. D. ten Haaf, Alberto Bordin, Sasa Gazibegovic, Ghada Badawy, Erik P. A. M. Bakkers *et al.*, Singlet and triplet cooper pair splitting in superconducting-semiconducting hybrid nanowires, arXiv:2205.03458.

[74] See Supplemental Material at http://link.aps.org/supplemental/10.1103/PhysRevLett.129.267701, which includes (1) derivation of the effective Hamiltonian for quantum dots, (2) calculation of the analytic expressions for CAR and ECT, (3) numerical simulation of realistic nanowires, (4) calculation of resonant current in three-terminal junctions.

[75] Fernando Domínguez and Alfredo Levy Yeyati, Quantum interference in a cooper pair splitter: The three sites model, Physica (Amsterdam) **75E**, 322 (2016).

[76] For clear illustration, we assume a constant spin-orbit coupling strength α_R throughout the nanowire in the main text. Actually, all the calculations and conclusions carry over to the more general scenarios of a spatially varying $\alpha_R(x)$, with only a minimal substitution of $k_{\mathrm{SO}}L \to \int_{x_l}^{x_r} k_{\mathrm{SO}}(x')dx'$.

[77] Tudor D. Stanescu and Sankar Das Sarma, Proximity-induced low-energy renormalization in hybrid semiconductor-superconductor Majorana structures, Phys. Rev. B **96**, 014510 (2017).

[78] J. J. Sakurai and J. Napolitano, *Modern Quantum Mechanics*, 2nd ed. (Addison-Wesley, San Francisco, CA, 2011).

[79] R. Hanson, L. M. K. Vandersypen, L. H. Willems van Beveren, J. M. Elzerman, I. T. Vink, and L. P. Kouwenhoven, Semiconductor few-electron quantum dot operated as a bipolar spin filter, Phys. Rev. B **70**, 241304(R) (2004).

[80] Jouri D. S. Bommer, Hao Zhang, Önder Gül, Bas Nijholt, Michael Wimmer, Filipp N. Rybakov, Julien Garaud, Donjan Rodic, Egor Babaev, Matthias Troyer, Diana Car, Sébastien R. Plissard, Erik P. A. M. Bakkers, Kenji Watanabe, Takashi Taniguchi, and Leo P. Kouwenhoven, Spin-Orbit Protection of Induced Superconductivity in Majorana Nanowires, Phys. Rev. Lett. **122**, 187702 (2019).

[81] Tom Dvir, Guanzhong Wang, Nick van Loo, Chun-Xiao Liu, Grzegorz P. Mazur, Alberto Bordin, Sebastiaan L. D. ten Haaf, Ji-Yin Wang, David van Driel, Francesco Zatelli *et al.*, Realization of a minimal Kitaev chain in coupled quantum dots, arXiv:2206.08045.